Itinerant ferromagnetism in heterostructured C/BN nanotubes

Jin Choi,[1] Yong-Hyun Kim,[1] K. J. Chang,[1] and David Tománek[2]
[1]*Department of Physics, Korea Advanced Institute of Science and Technology, Taejon 305-701, Korea*
[2]*Department of Physics and Astronomy, Michigan State University, East Lansing, Michigan 48824-1116*
(Received 20 November 2002; published 26 March 2003)

Using *ab initio* local spin-density-functional formalism, we study the occurrence of spin polarization in quasi-one-dimensional heterostructured C/BN nanotubes. At the zigzag boundary connecting carbon and boron nitride segments of tubes, we find atomiclike states that acquire magnetization when partly filled. Whereas individual C/BN heterojunctions can be used to spin-polarize electrons during transport, periodic arrangements of heterojunctions in doped systems can lead to the formation of a one-dimensional itinerant ferromagnetic state.

DOI: 10.1103/PhysRevB.67.125421 PACS number(s): 73.22.−f, 71.15.Nc, 75.70.Cn, 81.07.De

Following the recent discovery of ferromagnetism at room temperature in an all-carbon system consisting of polymerized C_{60},[1] there has been increased interest in magnetism in metal-free systems. Even though this finding is a significant step in the long-standing search for novel high-temperature magnets,[2] the observed magnetization, corresponding to less than an unpaired spin per thousand atoms, is too small. The origin of this magnetism is still unclear, and possibly linked to defects. This agrees with recent predictions of magnetism at the edge of graphene sheets and in BN/C heterosheets with somewhat artificial interface geometry.[3,4] Here we introduce heterostructured C/BN nanotubes with no undercoordinated atoms as a novel magnetic system with a magnetization a few hundred times larger than that of polymerized C_{60}.

Nanotubes of carbon, BN, BC_3, BC_2N and other stoichiometries have been synthesized successfully.[5–9] Experimental data indicate that these millimeter long, yet only nanometer wide quasi-1D nanostructures[10] cover the entire range from a metallic to an insulating behavior. Their electronic properties can be understood in terms of diameter, chirality, and elemental composition.[11,12] So far, there have been neither experimental indications nor theoretical predictions for the existence of magnetism in nanotubes. Here we study nanotubes consisting of hexagonal BN and C sheets seamlessly connected to form hollow cylinders. When adequately doped, these systems show, as we discuss in the following, magnetic behavior. The *p*-orbital ferromagnetism that we find follows, as we will show, the atomic Hund's rule in analogy to *d*-orbital magnetism in transition metals.

Our theoretical study of magnetism in C/BN nanotubes is based on the local spin-density-functional formalism (LSDA).[13] We use *ab initio* pseudopotentials[14] and the Ceperley-Alder exchange-correlation functional for the local spin density.[15] In our supercell calculations, we alternatively use two kinds of basis sets, namely, plane waves and a real-space grid, depending on the problem size. In both cases, we use a kinetic-energy cutoff of 36 Ry, and find our results to be independent of the basis used. Testing convergence with a higher energy cutoff of 49 Ry, we find the energy difference between ferromagnetic and nonmagnetic solutions to change by less than 1 meV. In plane-wave calculations, we sample the irreducible Brillouin zone by 5–25 **k**-points along the tube axis. In the real-space multigrid scheme, used for large unit cells, the Kohn-Sham matrix elements are evaluated at the Γ point only.[16]

Our calculation is carried out in a three-dimensional lattice with tetragonal unit cells. The intertube distance of 1.32 nm implies an interwall separation exceeding 0.6 nm, effectively decoupling the tubes. In view of the similarity between the bond lengths of 0.144 nm in narrow carbon nanotubes[17] and 0.145 nm in BN nanotubes,[18] we use 0.144 nm for the interatomic distances in the composite systems.

We primarily concentrate on the zigzag border between graphite and BN segments of the heterostructured nanotubes. At this interface, strongly localized states close to the Fermi level have been found in the planar geometry.[3] The occurrence of zigzag borders in C/BN nanotubes is also very likely due to the preferential zigzag growth of BN and C/BN nanotubes.[9,8,19] The energetically favorable phase separation of graphite and BN regions has been established both experimentally and theoretically.[20,21] We choose two representative extreme configurations for the zigzag border, which we display in Fig. 1. In Fig. 1(a) we show the (5,5) armchair nanotube, where the zigzag border runs along the tube axis. In Figs. 1(b) and 1(c) we depict the (9,0) zigzag nanotube, where a zigzag interface connects axial segments of different length. We classify them as $C_i(BN)_j$, where i and j denote the numbers of C and BN zigzag rings in the primitive cell, respectively.

The calculated band structures for the armchair C/BN nanotube and the zigzag $C_i(BN)_i$, $i=1,2$, nanotubes are shown in Fig. 2. As in perfect C and BN nanotubes, states near the Fermi level are derived from *p* orbitals. Our LSDA results indicate that all three geometries are nonmagnetic. Even though the armchair nanotube is metallic and shows a flat band that induces a large density of states at the Fermi level, we find no ferromagnetic solution there. The electronic structure is very similar to that found in C/BN heterosheets with the straight border,[3] which also are nonmagnetic. The undoped zigzag nanotubes show no magnetic solution due to the fundamental band-gap exceeding 0.5 eV, implying that all electrons are paired. As we discuss in the following, doping may change this fact dramatically.

The electronic structure of heterostructured zigzag nanotubes is very different from that of armchair tubes. The pris-

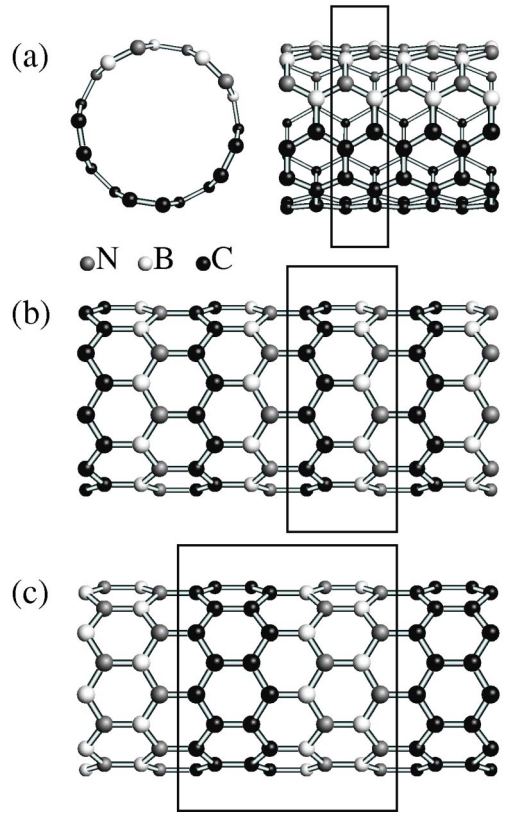

FIG. 1. Ball-and-stick models of heterostructured C/BN nanotubes. (5,5) armchair nanotube with axially connected contiguous carbon and BN regions (a). (9,0) zigzag $C_1(BN)_1$ (b), and $C_2(BN)_2$ (c) nanotubes. The boxes represent the supercells.

tine (9,0) BN nanotube has a large fundamental gap of about 4 eV,[18] whereas the (9,0) carbon nanotube has a small band gap of less than 0.1 eV, caused by *s*-*p* hybridization.[17] In the composite C/BN system, the Fermi levels of the segments, located at the mid-gap, are expected to align. Consequently, states in the vicinity of the Fermi level of heterostructured systems all originate from the carbon segments. In Fig. 2(b), we also note that the additional quantization due to the finite length of the carbon segment increases the fundamental gap of the $C_1(BN)_1$ heterostructure to about 2 eV from the initial 0.1 eV value in the infinite carbon nanotube.

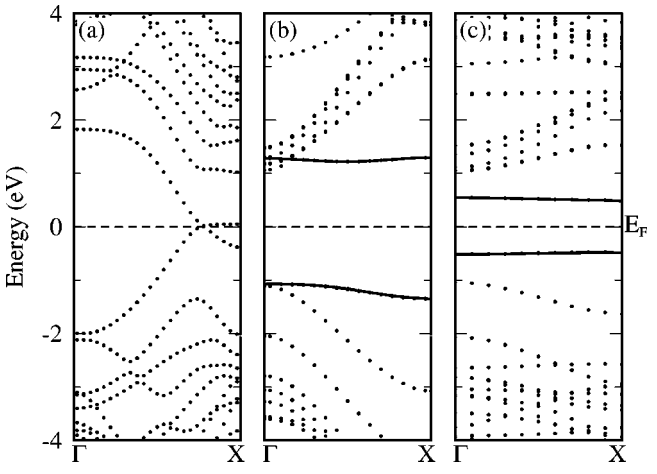

FIG. 2. Band structure of the (5,5) C/BN nanotube (a), the (9,0) $C_1(BN)_1$ (b), and $C_2(BN)_2$ (c) nanotubes. The Fermi level is set to 0 eV. The solid lines depict the flat, defectlike border states.

A second important feature found in zigzag tubes is the occurrence of very flat bands near the Fermi level, shown in Figs. 2(b) and 2(c), which remain nearly dispersionless over the entire Brillouin zone. From their charge density distribution, we know that the occupied flat bands are associated with the C—B bonding configuration and the unoccupied flat bands with the C—N antibonding configuration. Consequently, these states have the character of defect states at the boundary of the BN and carbon regions. The separation between these boundary states depends on the strength of the interaction between the different atomic species and the unit cell size. It is found to be 2.3 eV for $C_1(BN)_1$, 0.9 eV for $C_2(BN)_2$, and 1.3 eV for $C_3(BN)_1$. As we will show in the following, these boundary states may develop an interesting behavior when partly filled due to doping.

The degeneracy of the flat bands, including the spin degrees of freedom, is due to the absence of chirality in zigzag nanotubes. The spatial localization and degeneracy of the border states is, in some sense, analogous to that of transition metals, where partly filled, localized *d* states cause magnetism described by Hund's rules. In the superlattice, we find that the border states play the same role as localized *d* orbitals in a metal lattice, thus causing a similar magnetic behavior.

The dispersion of the flat bands depends on the unit cell size in the supercell geometry. We find them to be 0.27 eV wide in $C_1(BN)_1$ due to the large overlap of the border state wave functions across the short unit cell, but only 0.05 eV wide in $C_2(BN)_2$ with twice the unit cell size. We thus expect a spin polarization of the boundary states in doped $C_2(BN)_2$, similar to isolated atoms or quantum dots, giving rise to paramagnetism. In doped $C_1(BN)_1$, itinerant ferromagnetism should occur in analogy to *d*-orbital ferromagnetism in transition metals.

To study the magnetic ordering, we have performed extensive LSDA calculations for doped $C_i(BN)_j$ zigzag nanotubes with $1 \leqslant \{i,j\} \leqslant 7$. We found our results to be consistent with Hund's rule-type magnetic ordering, independent of the carrier type and the method used to model the flat band doping. Since the flat bands located in the valence-band and the conduction band region are both associated with the border states, both electron and hole doping should induce spin polarization. We model doping by three independent methods, namely, adjusting the charge neutrality level, selectively substituting B or N atoms for carbon atoms, and placing K atoms along the nanotube axis. Our results are found to be independent of the particular doping method. In particular, we find that not even substitutional doping can change the character of the localized border states.

Since the fourfold degenerate flat bands dominate the density of states closest to the Fermi level, Hund's rule-type effect is maximized by electron or hole doping with approximately two carriers per unit cell. Our total energy calculation shows that the ferromagnetic Kohn-Sham solution is more stable by 1.0 eV per unit cell than the nonmagnetic solution

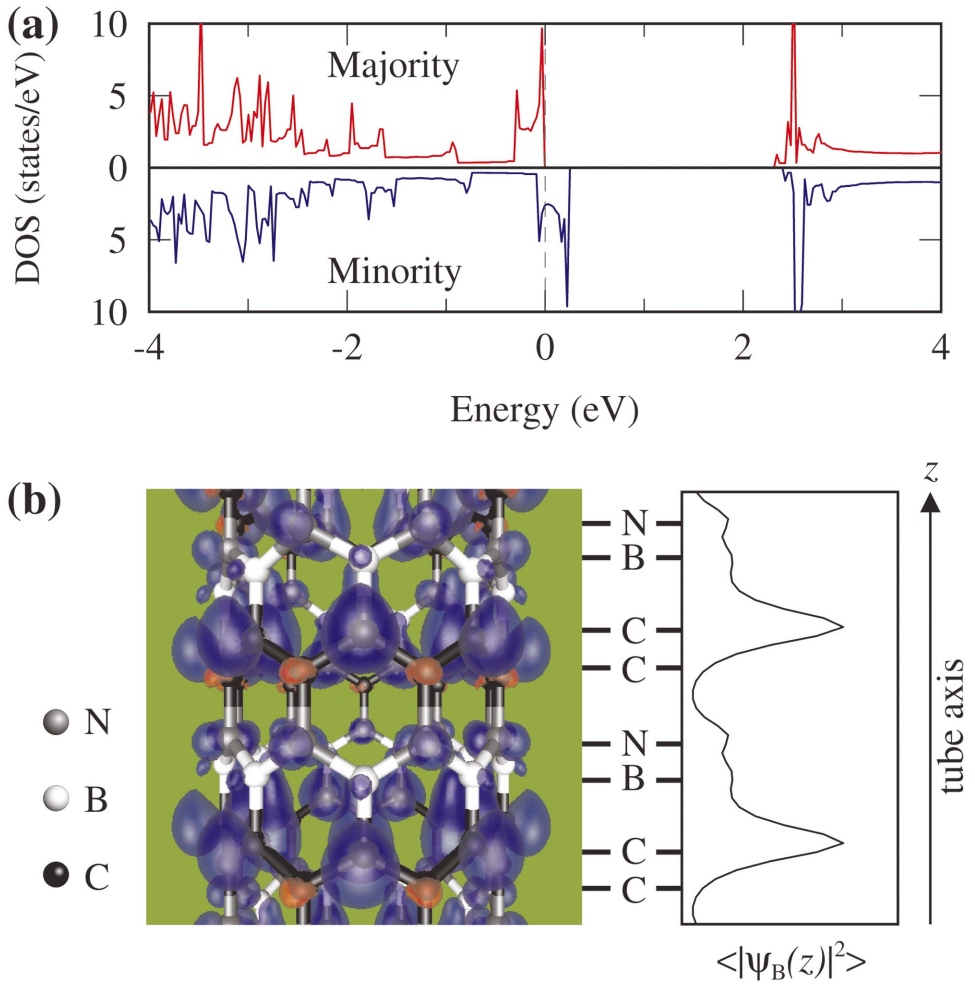

FIG. 3. (Color) (a) Majority and minority spin densities of states of the (9,0) $C_1(BN)_1$ nanotube, with the Fermi level set to 0 eV. (b) Three-dimensional plot of the spin-polarization density $[n_{maj}(\mathbf{r})-n_{min}(\mathbf{r})]$, superposed with the corresponding ball-and-stick model of the structure. The blue (red) clouds represent regions of majority (minority) spin-densities exceeding 4.0×10^{-2} electrons/nm^3 (2.5×10^{-2} electrons/nm^3). The charge-density associated with the border states, $\langle|\psi_B(z)|^2\rangle$, averaged normal to the tube axis, is shown in the right panel.

for the unrelaxed $C_1(BN)_1$ nanotube doped by two holes. This energy difference reduces to about 50 meV per unit cell upon full structural relaxation, with little effect on the band structure. A follow-up calculation with twice the unit cell size indicated that an imposed antiferromagnetic state would be even less stable than the nonmagnetic state. In the relaxed system, we find the C—C, B—N, C—N, and C—B bond lengths to be 0.142, 0.145, 0.135, and 0.155 nm, respectively, in good agreement with previous calculations.[18,22]

The spatial and energy distributions of the spin carriers in the $C_1(BN)_1$ system is shown in Fig. 3. Figure 3(a) displays the majority and minority spin densities of states of the hole-doped $C_1(BN)_1$ nanotube, which reflect the onset of magnetic ordering. Occurrence of magnetism in this system is quite unexpected, since densities of *s* and *p* derived states are usually quite low. The spatial distribution of the spin-polarization density $[n_{maj}(\mathbf{r})-n_{min}(\mathbf{r})]$, where n_{maj} (n_{min}) is the charge density of the majority (minority) spin, is depicted in the left-hand panel of Fig. 3(b). The right-hand panel shows the charge-density associated with the border states, $\langle|\psi_B(z)|^2\rangle$, averaged normal to the tube axis. The atomic positions along the *z* axis of the tube are common to both panels, as indicated by the labels.

According to Fig. 3(a), the $C_1(BN)_1$ nanotube, doped by two holes, acquires a net spin of $1.65\mu_B$ per unit cell. The reduction of the net charge transferred to the flat valence band and the corresponding change of the magnetic moment results from the fractional population of the carbon-derived bands in the vicinity of the Fermi level.[23] The charge distribution associated with the spin-polarized flat bands is shown in the right panel of Fig. 3(b). We observe that these states, although localized at the C/BN interface region, show a substantial overlap to induce magnetic ordering. As seen in the left panel of Fig. 3(b), the majority spin charge density is mostly localized on the C atoms associated with C—B bonds, whereas the minority spin density is mainly associated with C—N bonds. This results from the above-mentioned fact that the flat bands in the valence-band region are spatially localized at the C—B interface. The flat bands in the conduction-band region, which are depleted in the hole doped system, are at the C—N interface.

The localization of the spin density at the C/BN interface allows us to draw conclusions for other systems based on Hund's first rule. In the unrelaxed $C_2(BN)_2$ tube with twice the period of the preceding system, which we also doped with two holes per unit cell, our LSDA calculations indicate that formation of localized spin-polarized border states is energetically preferred by 35 meV per unit cell with respect to the non-spin-polarized solution. Full structural relaxation reduces this value to 30 meV. The 20 meV difference between the 30 meV value in $C_2(BN)_2$ and the 50 meV value in $C_1(BN)_1$ can be attributed to the overlap between the border states in the latter system, which lies at the origin of ferromagnetic ordering. Hence we find one-dimensional ferromagnetic ordering to be strongly favored in a superlattice with small unit cells, where the border states show a significant overlap. In systems with well separated heterojunctions, where the border states show a much smaller overlap, we may expect paramagnetism. In the following, we focus on the electronic structure of an individual C/BN heterojunction.

Since the electronic structure of the C/BN heterostructure depends strongly on the size of the unit cell, as seen from the comparison between Figs. 2(b) and 2(c), we use 144-atom large unit cells, which are sampled by a real-space grid at $\mathbf{k}=\Gamma$. The atomic arrangements in the $C_2(BN)_6$, $C_4(BN)_4$, $C_6(BN)_2$, and $C_7(BN)_1$ superlattices, with a constant unit cell size but a sequentially changing thickness of the individual segments, are shown in Fig. 4, together with the corresponding densities of states. In all geometries, we can identify the border states based on charge-density distribution and label them by arrows in the densities of states.

Due to the smallest overlap between the valence and conduction border states in $C_4(BN)_4$, with equally thick BN and carbon segments, we expect the separation of their energy eigenvalues for systems with well-separated borders to lie close to the 0.5 eV value shown in Fig. 4(b). This value increases in $C_2(BN)_6$ of Fig. 4(a) and $C_6(BN)_2$ of Fig. 4(c), where either the BN or the carbon segment becomes much shorter, thus increasing the overlap. The gradual approach of the carbon states to the Fermi level can be observed in the sequence of Figs. 4(a) to 4(d), as the quantization in the finite carbon segments gradually becomes less important.

In an isolated junction connecting infinitely long BN and carbon segments, we thus expect one border state embedded in a continuum of carbon states close to the Fermi level. Appropriate doping should then induce a spin polarization of the junction. An intriguing consequence arises from our prediction, when considering a device consisting of a narrow BN segment sandwiched in an otherwise perfect conducting carbon nanotube, similar to the geometry of Fig. 4(d). We postulate that spin unpolarized electrons, injected from one side of the carbon nanotube, should become spin polarized when passing through the junction.

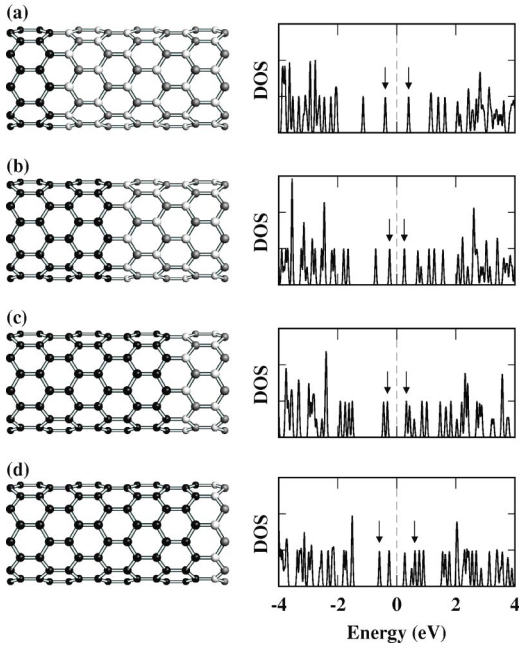

FIG. 4. Supercell geometries for the (9,0) (a) $C_2(BN)_6$, (b) $C_4(BN)_4$, (c) $C_6(BN)_2$, and (d) $C_7(BN)_1$ nanotubes. The corresponding densities of states are given in arbitrary units, and the Fermi level is set to 0 eV. The border states are marked by arrows.

In conclusion, we used local spin-density-functional calculations to study the occurrence of magnetism in quasi-one-dimensional heterostructured C/BN nanotubes free of metallic impurities. At the zigzag boundary connecting carbon and boron nitride segments of tubes, we found atomiclike states that acquire magnetization when partly filled. Whereas individual C/BN heterojunctions can be used to spin polarize electrons during transport, periodic arrangements of heterojunctions in doped systems can lead to the formation of a one-dimensional itinerant ferromagnetic state.

This work was supported by the QSRC at Dongguk University and the supercomputing center at KISTI. D.T. acknowledges support by the Korean IMT-2000 ''Molecular Logic Devices'' and the BK21 program, as well as the hospitality of Seoul National University.

[1] T.L. Makarova, B. Sundqvist, R. Höhne, P. Esquinazi, Y. Kopelevich, P. Scharff, V.A. Davydov, L.S. Kashevarova, and A.V. Rakhmanina, Nature (London) **413**, 716 (2001).

[2] F. Palacio, Nature (London) **413**, 690 (2001), and references therein.

[3] S. Okada, M. Igami, K. Nakada, and A. Oshiyama, Phys. Rev. B **62**, 9896 (2000).

[4] S. Okada and A. Oshiyama, Phys. Rev. Lett. **87**, 146803 (2001).

[5] S. Iijima, Nature (London) **354**, 56 (1991).

[6] M. S. Dresselhaus, G. Dresselhaus, and P. C. Eklund, *Science of Fullerenes and Carbon Nanotubes* (Academic Press Inc., 1996 San Diego), and references therein.

[7] N.G. Chopra, R. J. Luyken, K. Cherrey, V. H. Crespi, M. L. Cohen, S. G. Louie, and A. Zettl, Science **269**, 966 (1995).

[8] A. Loiseau, F. Willaime, N. Demoncy, G. Hug, and H. Pascard, Phys. Rev. Lett. **76**, 4737 (1996).

[9] D. Golberg, Y. Bando, W. Han, K. Kurashima, and T. Sato, Chem. Phys. Lett. **308**, 337 (1999).
[10] C. Dekker, Phys. Today **52**(5), 22 (1999).
[11] N. Hamada, S.I. Sawada, and A. Oshiyama, Phys. Rev. Lett. **68**, 1579 (1992).
[12] X. Blase, A. Rubio, S.G. Louie, and M.L. Cohen, Phys. Rev. B **51**, 6868 (1995).
[13] J.P. Perdew and A. Zunger, Phys. Rev. B **23**, 5048 (1981).
[14] N. Troullier and J.L. Martins, Phys. Rev. B **43**, 1993 (1991).
[15] D.M. Ceperley and B.J. Alder, Phys. Rev. Lett. **45**, 566 (1980).
[16] Y.-G. Jin, J.-W. Jeong, and K.J. Chang, Physica B **273**, 1003 (1999).
[17] C.-J. Park, Y.-H. Kim, and K.J. Chang, Phys. Rev. B **60**, 10 656 (1999).
[18] Y.-H. Kim, K.J. Chang, and S.G. Louie, Phys. Rev. B **63**, 205408 (2001).
[19] X. Blase, A. De Vita, J.-C. Charlier, and R. Car, Phys. Rev. Lett. **80**, 1666 (1998).
[20] K. Suenaga, C. Colliex, N. Demoncy, A. Loiseau, H. Pascard, and F. Willaime, Science **278**, 653 (1997); Y. Zhang, H. Gu, K. Suenaga, and S. Iijima, Chem. Phys. Lett. **279**, 264 (1997); Ph. Kohler-Redlich, H. W. Kroto, and D. R. M. Walton, **310**, 459 (1999).
[21] D.L. Carroll, Ph. Redlich, X. Blase, J.-C. Charlier, S. Curran, P. M. Ajayan, S. Roth, and M. Rühle, Phys. Rev. Lett. **81**, 2332 (1998); X. Blase, J.-C. Charlier, A. De, and R. Car, Appl. Phys. A: Mater. Sci. Process. **A68**, 293 (1999).
[22] X. Blase, J.-C. Charlier, A. De Vita, and R. Car, Appl. Phys. Lett. **70**, 197 (1997).
[23] A maximum moment of $2.0\mu_B$ can be achieved by further modifying the doping level.